DOI 10.1007/s11182-018-1337-2

Russian Physics Journal, Vol. 60, No. 12, April, 2018 (Russian Original No. 12, December, 2017)

FIRST-PRINCIPLES AND THERMODYNAMIC SIMULATION OF ELASTIC STRESS EFFECT ON ENERGY OF HYDROGEN DISSOLUTION IN ALPHA IRON

M. S. Rakitin, A. A. Mirzoev, and D. A. Mirzaev

UDC 538.95:544.032.3

Mobile hydrogen, when dissolving in metals, redistributes due to the density gradients and elastic stresses, and enables destruction processes or phase transformations in local volumes of a solvent metal. It is rather important in solid state physics to investigate these interactions. The first-principle calculations performed in terms of the density functional theory, are used for thermodynamic simulation of the elastic stress effect on the energy of hydrogen dissolution in α-Fe crystal lattice. The paper presents investigations of the total energy of Fe–H *system depending on the lattice parameter. As a result, the relation is obtained between the hydrogen dissolution energy and stress. A good agreement is shown between the existing data and simulation results. The extended equation is suggested for the chemical potential of hydrogen atom in iron within the local stress field. Two parameters affecting the hydrogen distribution are compared, namely local stress and phase transformations.*

Keywords: first-principle calculation, dissolution energy, stress effect, Fe–H, flake, phase transformation.

INTRODUCTION

Even the fact that hydrogen (H), when dissolving, increases the volume of iron specimens, raises the suggestion that the external stresses along with the gas pressure affect H solubility because the external force resistance is observed during the specimen expansion [1–3]. The value of

$$\bar{V}_{\mathrm{H}} = \frac{\partial V}{\partial n_{\mathrm{H}}} \tag{1}$$

is called a partial molar volume of hydrogen. According to works [1, 4], H volume equals 2 cm^3/mol. However, Shtremel' in [1] mentioned a wide spread in experimental values of this volume. Therefore, one of the most important problems of our studies is to precisely detect the hydrogen dissolution energy at a different hydrostatic pressure as well as its partial molar volume $\bar{V}_{\mathrm{H}}$ using the first-principle computer simulations. The obtained data allow us to perform successive thermodynamic calculations of the external stress effect on H dissolution energy in BCC iron.

Hydrogen dissolved in quenched heavy steel specimens, is exposed to internal stresses which occur due to uneven cooling of their different parts [5]. A nonuniform temperature field causes a inhomogeneous stress field which, in turn, leads to either a growth or reduction in H concentration in adjacent areas, thereby intensifying the formation of hydrogen cracks (flakes). Therefore, it is very crucial to analyze the stress effect on H solubility. Moreover, it is interesting to compare the hydrogen distributions in differently stressed areas and residual austenite areas.

National Research South Ural State University, Chelyabinsk, Russia, e-mail: maxim.rakitin@gmail.com; mirzoev@physics.susu.ac.ru; mirzaevda@susu.ac.ru. Translated from Izvestiya Vysshikh Uchebnykh Zavedenii, Fizika, No. 12, pp. 76–82, December, 2017. Original article submitted April 25, 2017; revision submitted August 29, 2017.

SIMULATION METHODOLOGY

The use of highly accurate calculation methods in theoretical studies of hydrogen in metals has become possible with the advent of computers and the development of first-principles calculation methods of solid melt properties. In terms of the density functional theory, the linearized augmented planewave (LAPW) method is among the most accurate methods of calculating the electronic structure of crystals. We use WIEN2k software package as an implementation of this method [6].

A LAPW basis set is used for simulations. Integration over the Brillouin zone uses a 4×4×4 points sampling of the primitive cell in *k*-space. Calculations are considered to be convergent when the supercell total energy is stabilized with the accuracy of up to 10^{-4} Ry. Benchmark calculations with WIEN2k software package show that the approximation of generalized density gradient [7] is a more accurate method as compared to that of the local spin density. Therefore, we choose a GGA-PBE96 exchange-correlation potential [8] which best describes the electron subsystem of the studied structures. In all calculations we use a BCC lattice with iron atoms in its points. The lattice parameter is selected to be equal to 5.41 atomic units, which corresponds to α-Fe experimental value. The spherical radius R_{mt} is determined automatically during calculations.

Using these approximations, the total energy of Fe–H system is calculated with regard to the spin polarization within the density functional theory. A supercell with H atom in a tetrahedral pore within the BCC cell, consists of 54 iron atoms. The calculation accuracy is evaluated through the binding energy, the main parameter of the interaction between atomic hydrogen and iron atoms. However, it is impossible to experimentally measure the binding energy. Usually, it is calculated from [9]:

$$\Delta E_{\text{sol}}(\text{H}) = \frac{1}{2} E_{\text{dis}}(\text{H}_2) - E_b(\text{H}), \tag{2}$$

where $\Delta E_{\text{sol}}(\text{H})$ is the energy of hydrogen dissolution in metal; $E_{\text{dis}}(\text{H}_2)$ is the dissociation energy of H molecule; $E_{\text{b}}(\text{H})$ is the binding energy of H atom in metal. The latter is used to carry out qualitative evaluations in this work.

Let us give here thermodynamic values for the estimation of H dissolution energy in iron. According to [9], $E_{\text{dis}}(\text{H}_2)$ = 453.6 kJ/mol, $\Delta E_{\text{sol}}(\text{H}) = \Delta H$ = –6.5 kcal/mol, where ΔH is molar enthalpy of H dissolution. Deriving the binding energy $E_{\text{b}}(\text{H})$ from Eq. (2) and substituting in it values for $\Delta E_{\text{sol}}(\text{H})$ and $E_{\text{dis}}(\text{H}_2)$, we obtain $E_{\text{b}}(\text{H})$ = 0.1936 Ry/atom.

Computer simulation implies the calculation of H binding energy in iron as [9]

$$E_{\text{b}}(\text{H}) = E(\text{Fe}_n\text{H}) - E(\text{Fe}_n), \tag{3}$$

where $E_{\text{b}}(\text{H})$ is the binding energy of H atom in BCC iron crystal; $E(\text{Fe}_n\text{H})$ and $E(\text{Fe}_n)$ are total energies of Fe_nH and Fe_n systems, respectively; n is the size of a supercell. Fe_n lattice has a body-centered cubic crystal system, without distortions.

RESULTS AND DISCUSSION

Figure 1 plots the first-principle calculation results of the total energy of BCC supercell comprising 54 atoms of pure iron and iron with one interstitial H atom.

As can be seen from Fig. 1, the minimum values of the total energy correspond to the equilibrium values V_0 of the lattice parameters. The relative parameter deviation from the equilibrium value can be caused by the relative deformation of the lattice:

$$\varepsilon = \frac{1}{3}\frac{V - V_0}{V_0}.$$

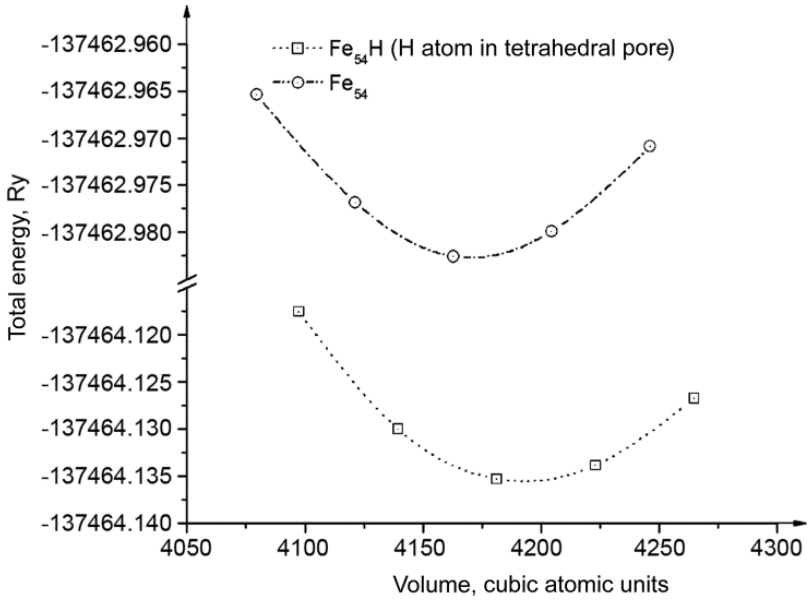

Fig. 1. Dependence between total energy and volume of Fe_{54} and $Fe_{54}H_1$ supercell.

Using Eqs (2) and (3), we can find the relation between the hydrogen dissolution energy and relative lattice deformation:

$$\Delta E_{\text{sol}}(\text{H}) = \frac{1}{2} E_{\text{dis}}(\text{H}_2) - E(\text{Fe}_{54}\text{H}_1) + E(\text{Fe}_{54}). \tag{4}$$

Clarifications and amendments

Computer simulation of the hydrostatic stress effect on the dissolution energy in iron is underlined by the following thermodynamic ideas. Let us consider the energy of a specimen comprising δn_1 iron moles and having the volume of

$$V_0 = \bar{V}_{\text{Fe}} \cdot \delta n_1, \tag{5}$$

where $\bar{V}_{\text{Fe}}$ is the partial molar volume of iron which is considered to be the same both for a dilute H solution and pure iron. If $E_0 \cdot \delta n_1$ denotes the iron energy in the equilibrium, stress-free state, E_0 then denotes the energy of one iron mole. In the case of uniform tensile stresses, we have $\sigma_{11} = \sigma_{22} = \sigma_{33} = -p$, where p is the hydrostatic pressure. Owing to the symmetry of the cubic lattice, percentage extensions of ε_{11}, ε_{22} and ε_{33} are identical, while shear deformations are absent. A relative change in the volume is $\frac{\delta V}{V} = \varepsilon_{11} + \varepsilon_{22} + \varepsilon_{33} = 3\varepsilon_{11}$, and the density of the elastic energy of

$$U = \frac{1}{2} K \left(\frac{\delta V}{V} \right)^2 \tag{6}$$

is determined by the bulk modulus K. In accordance with the work of Shtremel' [10], $K = \frac{1}{3} E$, where E is the normal elastic modulus along <100> direction, and the respective stress is $\sigma_{11} = E\varepsilon_{11}$. Hence, in terms of the uniform tensile stress, the elastic energy density can be written as

$$U = \frac{9}{2}\frac{\sigma^2}{E} = 3\frac{\sigma^2}{2K}. \quad (7)$$

For the total elastic energy we obtain $3\frac{\sigma^2}{2K}V_0$, whereas the total energy of the uniform tensile stress in the iron specimen represented in Eq. (4) as $E(\mathrm{Fe}_{54})$, is defined as

$$E(\mathrm{Fe}_{54}) = \left(E_0 + \frac{3}{2}\frac{\sigma^2}{K}\right)V_{\mathrm{Fe}} \cdot \delta n_1. \quad (8)$$

Next, we place $\delta n_2 = \delta n_{\mathrm{H}}$ hydrogen moles in the iron lattice. The impurity H atom being located in the tetrahedral pore of solvent, disturbs the electron density. This leads to changes in interatomic spacing, interaction potentials and their derivatives – binding forces. After the disturbance averaging over the lattice, two macroscopic effects are observed, namely: changes in the lattice parameter a and the elastic modulus both proportional to H atomic fraction x_{H}. Therefore, we observe two dimensionless characteristics [1], such as the coefficient of H concentration expansion (Eq. (9)) and the relative bulk modulus (Eq. (10)). These characteristics are respectively described by the following equations:

$$u_{ll} = \frac{1}{\Omega}\frac{d\Omega}{dx_{\mathrm{H}}} = \sum_{i=1}^{3}\frac{1}{a_i}\frac{\partial a_i}{\partial x_{\mathrm{H}}}; \quad (9)$$

$$\varepsilon_K = \frac{1}{K}\frac{dK}{dx_{\mathrm{H}}}. \quad (10)$$

Partial molar volume and dissolution energy

As mentioned above, the value of $\Omega u_{ll} N_0$ denotes the partial molar volume $\bar{V}_{\mathrm{H}}$ of hydrogen. However, the calculation of this value using this relation, gives 0.4 cm^3/mol, whereas dilatometer investigations carried out by Gel'd and Ryabov [4, p. 287] showed that $\bar{V}_{\mathrm{H}} \approx 2.0$ cm^3/mol. There is virtually no information offered in the literature concerning the relative change in the iron bulk modulus during H dissolution.

When $N_0 \delta n_{\mathrm{H}}$ hydrogen atoms are introduced into the specimen, its volume increases by $\bar{V}_{\mathrm{H}}\delta n_{\mathrm{H}}$. Firstly, it results in $\frac{3\sigma^2}{2K}\bar{V}_{\mathrm{H}}\delta n_{\mathrm{H}}$ increase in the elastic energy of the specimen [11]. Secondly, the applied stress changes the volume by $\bar{V}_{\mathrm{H}}\sigma_{11}\delta n_{\mathrm{H}}$ which, in turn, decreases the energy of Fe–H system. Finally, the increase in the bulk modulus causes $-\frac{3\sigma^2}{2K}\left(\frac{1}{K}\frac{dK}{dx_{\mathrm{H}}}\right)\bar{V}_{\mathrm{H}}\delta n_{\mathrm{H}}$ energy reduction in $\bar{V}_{\mathrm{H}}\sigma_{11}\delta n_{\mathrm{H}}$ volume which contains hydrogen. Here the value in brackets denotes the relative change in the bulk modulus ε_K.

Similar to Eq. (8), let us calculate the total energy $\mathrm{Fe}_{54}\mathrm{H}_1$ of the supercell in a stress state:

$$\left(E_0(\mathrm{Fe}_{54}\mathrm{H}_1) + \frac{3}{2}\frac{\sigma_{11}^2}{K}\right)\bar{V}_{\mathrm{Fe}} \cdot \delta n_1 + \left(\frac{3}{2}\frac{\sigma_{11}^2}{K} - \frac{3}{2}\frac{\sigma_{11}^2}{K}\left(\frac{1}{K}\frac{dK}{dx_{\mathrm{H}}}\right) + \sigma_{11}\right)\bar{V}_{\mathrm{H}} \cdot \delta n_{\mathrm{H}}. \quad (11)$$

Now we can derive the dissolution energy for one H atom according to Eq. (4) ($\delta n_{\mathrm{H}} = 1/N_0$, where N_0 is Avogadro's number):

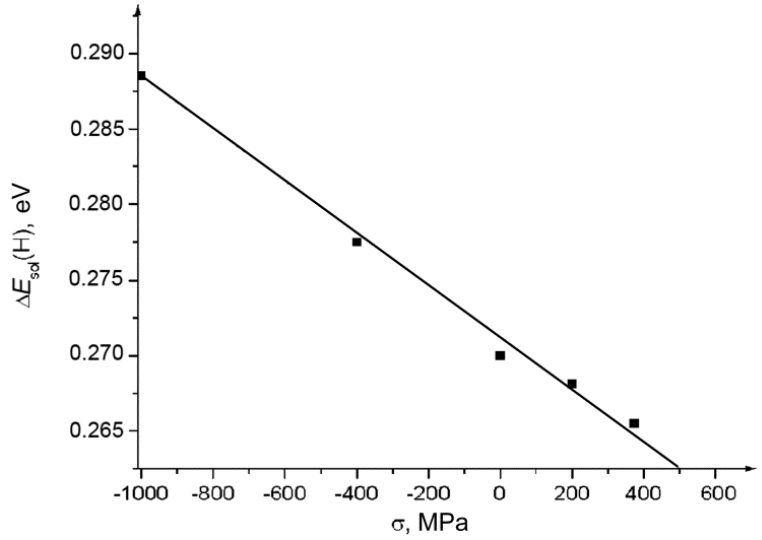

Fig. 2. Dependence between the energy of H dissolution $\Delta E_{\mathrm{sol}}(\mathrm{H})$ in α-Fe and external hydrostatic stress σ.

$$\Delta E_{\mathrm{sol}}(\mathrm{H}) = \frac{1}{2} E_{\mathrm{dis}}(\mathrm{H}_2) - E(\mathrm{Fe}_{54}\mathrm{H}_1) + E(\mathrm{Fe}_{54}) - \frac{\sigma \bar{V}_{\mathrm{H}}}{N_0}, \tag{12}$$

where $E(\mathrm{Fe}_{54}\mathrm{H}_1) - E(\mathrm{Fe}_{54})$ is the total energy difference for supercells in a stress-free state. Other summands in brackets in Eq. (11) are negligibly small. Actually, $\sigma_{11}/K \sim 2\cdot 10^{-4}$, where we use the experimental value of K = 162 GPa [10], while the relative change in the bulk modulus is not recorded in the experiment. According to Eq. (12), the dependence between the dissolution energy and the stress should be linear, the slope coefficient being $\bar{V}_{\mathrm{H}}/N_0$, *i.e.* equaling the partial volume of H atom. As can be seen from Fig. 2 which plots the first-principle calculation results of the dissolution energy depending on σ_{11}, this dependence is really close to linear. In view of the upper and the lower points, let us calculate the ratio of $\bar{V}_{\mathrm{H}}/N_0$:

$$\frac{\bar{V}_{\mathrm{H}}}{N_0} = \frac{(0.289 - 0.264)\cdot 1.602\cdot 10^{-19}\ \mathrm{J}}{(1023 + 362)\cdot 10^{6}\ \mathrm{Pa}} = 2.88\cdot 10^{-30}\ \frac{\mathrm{m}^3}{\mathrm{atom\,H}}. \tag{13}$$

From this we can derive the partial molar volume of hydrogen: $\bar{V}_{\mathrm{H}} = 17.7\cdot 10^{-7}$ m^3/mol = 1.77 cm^3/mol, which closely corresponds to data obtained in [1, 4], *i.e.* $\bar{V}_{\mathrm{H}} = 2$ cm^3/mol.

Thus, computer simulation of the uniform external stress effect on the energy of H dissolution and the partial molar volume gives the following results: $\bar{V}_{\mathrm{H}}$ = 1.77 cm^3/mol and ΔE_{sol} = 0.269 eV/atom = 26.0 kJ/mol. For comparison, let us provide the equation for hydrogen solubility C_{H} in α-Fe described in [4] using more accurate measurements:

$$C_{\mathrm{H}} = 47.534 \exp\left(-\frac{27.180\ (\mathrm{kJ/mol})}{RT}\right)\sqrt{p_{\mathrm{H}_2}}, \tag{14}$$

where p_{H_2} is the pressure of H vapor around the specimen. As is clear from Eq. (14), there is a good agreement between the experimental and simulated results on the energy of H dissolution in iron.

Chemical potential

Equation (12) relates to a situation when dissolved hydrogen is in the equilibrium state with H_2. However, it often enters the steel as early as it is molten. In the course of the specimen cooling which occurs at $p_{H_2} \approx 0$, the time of H release is much longer than that of cooling. Therefore, H solution in α-Fe turns to be strongly oversaturated. In such conditions, H atoms migrate inside the solid phase, and relaxation to the local equilibrium occurs depending on the relation between chemical potentials of H atoms at different points of the structure. In [12], we obtained the hydrogen chemical potential μ_H for the binary Fe–H alloy:

$$\mu_H = \mu_H^\circ + RT \ln \frac{x_H}{1 - x_H}, \tag{15}$$

where μ_H° is the chemical potential of hydrogen in a standard state of infinitely dilute solution; x_H is the atomic fraction of hydrogen in solution; the ratio $x_H/(1–x_H)$ is known as θ_H. In the uniaxial elastic stress field, the chemical potential μ_H° depends on the external hydrostatic stress σ [11]:

$$\mu_{0.1}^H = \mu_H^\circ + \frac{\sigma}{3}\bar{V}_H + \frac{\sigma^2}{2E}\bar{V}_H\left(1 - \frac{1}{E}\frac{dE}{dx_H}\right), \tag{16}$$

summands in brackets being small as compared to $\frac{\sigma}{3}\bar{V}_H$. In the case of the uniform external tension, the second summand is expressed by $\sigma\bar{V}_H$. We assume, that the specimen contains area I with tensile stress σ, and area II with compressive stress –σ. Between these two areas there is area III, in which $\sigma = 0$. Making chemical potentials equal, the local equilibrium is determined to be

$$RT \ln \frac{x_H^I}{x_H^{III}} = \bar{V}_H \frac{\sigma}{3}, \; RT \ln \frac{x_H^{II}}{x_H^{III}} = -\bar{V}_H \frac{\sigma}{3}. \tag{17}$$

For simplicity we assume that $T = 300$ K and $\sigma = 300$ MPa. The molar volume $\bar{V}_H = 2$ cm^3/mol $= 2 \cdot 10^{-6}$ m^3/mol. Then, $\frac{x_H^I}{x_H^{III}} = \exp\left(\frac{2 \cdot 300}{3 \cdot 8.314 \cdot 300}\right) = 1.083$, $\frac{x_H^{II}}{x_H^{III}} = 0.923$ and $\frac{x_H^I}{x_H^{II}} = 1.174$. When σ achieves values close to the yield stress of the steel, ~1000 MPa, we get $\frac{x_H^I}{x_H^{II}} = 1.706$, *i.e.* $\frac{x_H^I}{x_H^{II}}$ increases by 70%.

Another factor of H redistribution inside the crystal lattice is the existence of γ- and α-phases within a wide temperature range, in which austenite (γ-phase) transforms to ferrite, bainite, or martentsite (α-phase). With the ignorance of stresses, the local H equilibrium occurs due to a fast diffusion at the interphase boundary:

$$\mu_H^\alpha = \mu_H^\gamma = \frac{1}{2}\mu_{H_2}, \tag{18}$$

where μ_{H_2} is the chemical potential of H_2 molecules in gas phase which at pressure p_{H_2} are in the equilibrium with α- and γ-phases. Since $\mu_{H_2} = \mu_{H_2}^\circ + RT \ln p_{H_2}$ and $\mu_{H_2}^\circ$ is the chemical potential of H_2 in its standard gaseous state, p_{H_2} and $\mu_{H_2}^\circ$ are independent of the lattice type.

In the case of the equilibrium state of $[H]^\gamma \leftrightarrow \frac{1}{2}H_2$, we again derive from Eq. (15) the hydrogen chemical potential μ_H in γ-phase:

$$\mu_{\mathrm{H}}^{\gamma} = {}^{\circ}\mu_{\mathrm{H}}^{\gamma} + RT\ln\theta_{\mathrm{H}}^{\gamma} = \frac{1}{2}\mu_{\mathrm{H}_2}^{\circ} + \frac{1}{2}RT\ln p_{\mathrm{H}_2} \tag{19}$$

and

$$\ln\theta_{\mathrm{H}}^{\gamma} = \frac{1}{RT}\left(\frac{1}{2}\mu_{\mathrm{H}_2}^{\circ} - \frac{1}{2}RT\ln p_{\mathrm{H}_2} - {}^{\circ}\mu_{\mathrm{H}}^{\gamma}\right). \tag{20}$$

Analogously,

$$\ln\theta_{\mathrm{H}}^{\alpha} = \frac{1}{RT}\left(\frac{1}{2}\mu_{\mathrm{H}_2}^{\circ} - \frac{1}{2}RT\ln p_{\mathrm{H}_2} - {}^{\circ}\mu_{\mathrm{H}}^{\alpha}\right). \tag{21}$$

The difference of these values is

$$\ln\theta_{\mathrm{H}}^{\gamma} - \ln\theta_{\mathrm{H}}^{\alpha} = \ln\frac{\theta_{\mathrm{H}}^{\gamma}}{\theta_{\mathrm{H}}^{\alpha}} = \frac{{}^{\circ}\mu_{\mathrm{H}}^{\alpha} - {}^{\circ}\mu_{\mathrm{H}}^{\gamma}}{RT}. \tag{22}$$

On the strength of proportionality between the hydrogen mass fractions in α- and γ-phases and θ_{H} value, Eq. (22) can be written as

$$\ln\frac{C_{\mathrm{H}}^{\gamma}}{C_{\mathrm{H}}^{\alpha}} = \frac{{}^{\circ}\mu_{\mathrm{H}}^{\alpha} - {}^{\circ}\mu_{\mathrm{H}}^{\gamma}}{RT}. \tag{23}$$

Next, using Eq. (14) for H solubility in α-phase and the similar equation for γ-phase obtained in [4], we get H solubility in γ-iron:

$$C_{\mathrm{H}}^{\gamma} = 47.534\exp\left(-\frac{22628\ (\mathrm{J/mol})}{RT}\right)\sqrt{p_{\mathrm{H}_2}}, \tag{24}$$

we have

$$\frac{C_{\mathrm{H}}^{\gamma}}{C_{\mathrm{H}}^{\alpha}} = \exp\left(\frac{4552\ (\mathrm{J/mol})}{RT}\right). \tag{25}$$

From this we deduce $\frac{C_{\mathrm{H}}^{\gamma}}{C_{\mathrm{H}}^{\alpha}} = 3.00$ at 500 K; 3.93 at 400 K; 6.20 at 300 K and 15.4 at 200 K. Apparently, γ-phase will withdraw hydrogen from α-phase, thereby increasing the intrinsic H concentration. At temperatures approaching to room temperature, austenite transforms to martensite and delivers it captured hydrogen. Probably, this is the main cause of the flake nucleation. The formation of martensite enables the growth of the volume of its crystal lattice. Therefore, compressive stresses appear in transformed austenite. However, the stress influence is considerably lower than that of H solubility difference in α- and γ-phases, and cannot ensure the uniform hydrogen distribution.

CONCLUSIONS

1. The first-principle calculations showed that the dissolution energy of hydrogen in α-Fe decreased linearly with the increase of uniform tensile stresses.

2. The suggested dependence was used to compute the dissolution energy of hydrogen in unstressed α-Fe (26.0 kJ/mol) and its molar volume (1.77 cm^3/mol).

3. A comparison of causes for the nonuniformity of H atom distribution showed that the interphase boundary between austenite and martensite has a greater effect on the hydrogen redistribution than the non-uniform stress field occurred in heavy steel specimens.

This work was financially supported by Grant N 16-19-10252 from the Russian Science Foundation.

REFERENCES

1. M. A. Shtremel', Strength of Alloys. Pt. II: Lattice Defects [in Russian], MISiS, Moscow (1997).
2. G. Alefeld and J. Völkl (Eds.), Hydrogen in Metals [Russian translation], Mir, Moscow (1981).
3. Y. Fukai, The Metal-Hydrogen System. Heidelberg, Springer Verlag, Berlin (2005).
4. P. V. Gel'd and R. A. Ryabov, Hydrogen in Metals and Alloys [in Russian], Metallurgiya, Moscow (1974).
5. D. A. Mirzaev, A. D. Shaburov, and A. O. Chernyavskii, Vestnik Yuzhno-Ural'skogo gosudarstvennogo universiteta. Ser. Metallurgiya, **14**, No. 3, 40–45 (2014).
6. K. Schwarz, P. Blaha, and G. K.H. Madsen, Comput. Phys. Commun., **147**, 71–76 (2002).
7. J. P. Perdew, K. Burke, and M. Ernzerhof, Phys. Rev. Lett., **77**, 3865 (1996).
8. C. Elsasser, J. Zhu, S. G. Louie, *et al*. J. Phys.: Cond. Matter, **10**, 5081–5111 (1998).
9. D. E. Jiang and E. A. Carter, Phys. Rev. B, **70**, 064102 (2004).
10. M. A. Shtremel', Strength of Alloys. Pt. II: Lattice Defects [in Russian], MISiS, Moscow (1999)
11. J. C. M. Li, R. A. Oriani, and L. S. Darken, Z. Phys. Chem. Neue Folge, No. 49, 271–290 (1966).
12. D. A. Mirzaev, A. A. Mirzoev, I. V. Kashukov, and K. Yu. Okishev, Phys. Met. Metallogr., **108**, No. 5, 496-503 (2009).